Received: 14 May 2023 | Revised: 27 July 2023 | Accepted: 5 August 2023

DOI: 10.1002/eom2.12406

REVIEW

EcoMat FUNCTIONAL MATERIALS FOR GREEN ENERGY AND ENVIRONMENT WILEY

Unlocking the potential of metal halide perovskite thermoelectrics through electrical doping: A critical review

Yongjin Kim[1,2] | Hyeonmin Choi[1,2] | Jonghoon Lee[3] | Young-Kwang Jung[4] | Joonha Jung[1] | Jaeyoon Cho[1] | Takhee Lee[3,5] | Keehoon Kang[1,2,5]

[1]Department of Materials Science and Engineering, Seoul National University, Seoul, South Korea

[2]Research Institute of Advanced Materials (RIAM), Seoul National University, Seoul, South Korea

[3]Department of Physics and Astronomy, Seoul National University, Seoul, South Korea

[4]Department of Chemical Engineering and Biotechnology, University of Cambridge, Cambridge, UK

[5]Institute of Applied Physics, Seoul National University, Seoul, South Korea

Correspondence

Keehoon Kang, Department of Materials Science and Engineering, Seoul National University, Seoul 08826, Korea.
Email: keehoon.kang@snu.ac.kr

Takhee Lee, Department of Physics and Astronomy, and Institute of Applied Physics, Seoul National University, Seoul 08826, Korea.
Email: tlee@snu.ac.kr

Funding information

BrainLink Program, Grant/Award Number: 2022H1D3A3A01077343; Nano Material Technology Development Program, Grant/Award Number: 2021M3H4A1A02049651; National Research Foundation of Korea, Grant/Award Numbers: 2021R1A2C3004783, 2021R1C1C1010266; Seoul National University; Ministry of Science and ICT (MSIT) of Korea

Abstract

Over the past decade, metal halide perovskites (MHPs) have received great attention, triggered by the tremendous success of their record-breaking power conversion efficiency values in solar cells. Recently, there have been significant interests in fully utilizing their unique properties by exploring other device applications including thermoelectrics, which is promising due to their ultralow thermal conductivity and high mobility relative to their competitors among solution-processable materials. However, the performance of MHP thermoelectrics reported so far falls significantly short of theoretical predictions, as the doping levels achieved to date are typically below the optimum values for maximizing the thermoelectric power factor, indicating the need for effective electrical doping strategies. In this critical review, recent studies aimed at enhancing the thermoelectric properties of MHPs are discussed, with a focus on the relatively under-explored area of electrical doping in MHPs. The underlying charge transport mechanism and doping effect on transport are also examined. Finally, the challenges facing MHP thermoelectrics are highlighted, and potential research visions for achieving highly efficient thermoelectric conversion based on MHPs are offered.

KEYWORDS

charge transport, doping, electrical doping, metal halide perovskites, thermoelectrics

1 | INTRODUCTION

Metal halide perovskites (MHPs) have attracted tremendous attention in optoelectronic applications due to their outstanding properties such as high photoluminescence quantum yield (PLQY), high absorption coefficient, defect tolerance, tunable bandgap, and facile solution processing.[1–11] In just over a decade, solar cells based on MHPs have achieved an impressive 25.7% efficiency,[1] and green light-emitting diodes (LEDs) have reached a high

external quantum efficiency (EQE) of 28.9%,[10] demonstrating the potential of MHPs as a next-generation energy and display material. The most extensively studied structure is a three-dimensional (3D) structure, with the formula of ABX_3, where A is a monovalent organic/inorganic cation, B is a divalent metal cation, and X is a halide anion. Furthermore, MHPs with various low-dimensional structures, such as two-dimensional (2D) Ruddlesden-Popper (RP) phase ($A'_2A_{n-1}B_nX_{3n+1}$), and zero-dimensional (0D) structures (A_4BX_6, A_2BX_6, $A_3B_2X_5$, etc.), have also been widely studied, each possessing unique and crucial characteristics relevant to specific applications.[12–18]

In addition to their excellent optical properties, MHPs are known for their ultralow thermal conductivity,[19–22] which makes them promising materials for next-generation thermoelectric applications that convert thermal energy into electrical energy, enabling the use of waste heat. The "phonon glass electron crystal" structure of MHPs potentially enables efficient charge transport while minimizing heat transport,[23] resulting in both a high electrical conductivity and low thermal conductivity. Furthermore, MHPs exhibit a high Seebeck coefficient at room temperature, highlighting their exceptional ability to generate thermoelectric voltage based on temperature differences. This advantage, combined with their ultralow thermal conductivity and high charge carrier mobility, is expected to provide high thermoelectric performance.[19–21,24] Apart from their performance-related advantages, MHPs offer a cost-effective alternative to traditional inorganic thermoelectric materials due to their simple fabrication and low material costs, potentially driving more widespread adoption of thermoelectric technology. The material versatility of MHPs also allows for tailored performance based on specific application requirements, providing opportunities for further optimization.[17,18] Moreover, MHPs are expected to exhibit high thermoelectric conversion efficiency at close to room temperature, making them a crucial factor for the successful implementation of various wearable applications.[25,26]

As can be seen in Figure 1A, inorganic materials such as Bi_2Te_3,[27] PbTe,[28] SnSe,[29] Skutterudites,[30] and Half-Heusler compounds[31] have been the subject of extensive research as thermoelectric materials, but their commercialization has been hindered by several limitations including their high production cost, the toxicity of constituent elements, brittleness, and limited abundance. Although organic materials, represented by poly(3,4-ethylenedioxythiophene)-poly(styrenesulfonate) (PEDOT:PSS),[32] have also been explored for thermoelectrics, their performance is

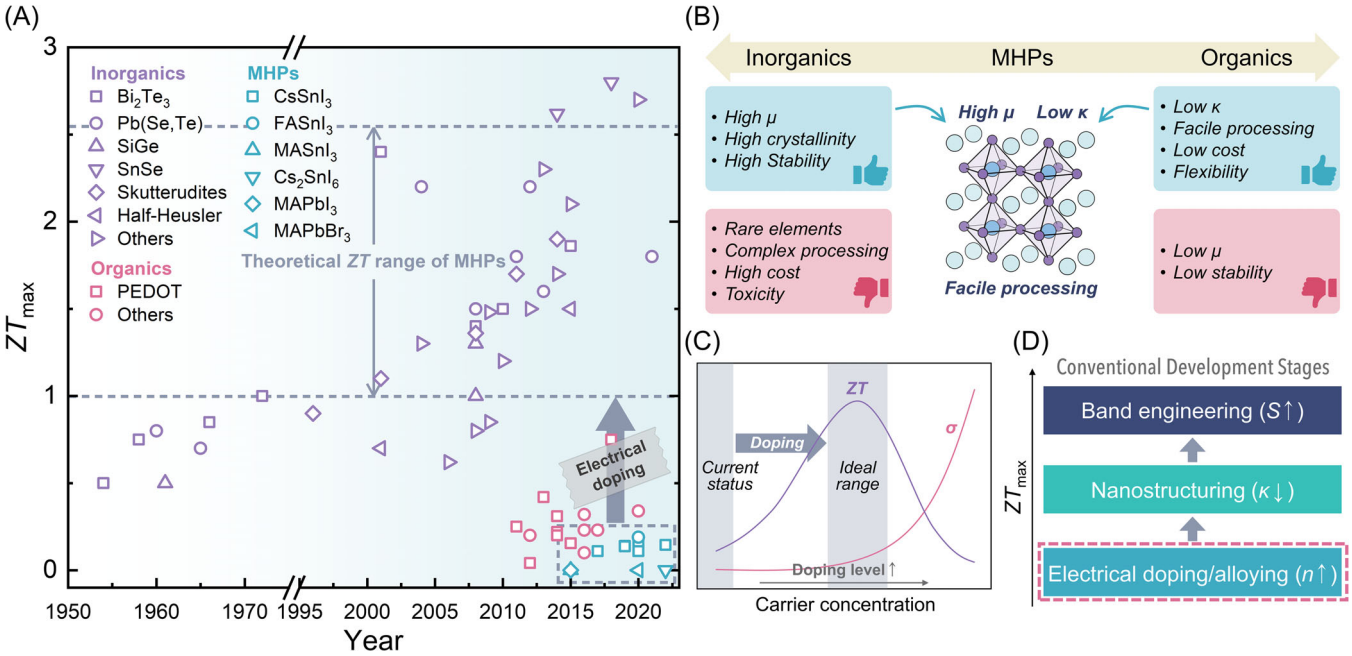

FIGURE 1 (A) Timeline and progress in thermoelectric conversion efficiency represented for conventional inorganic[27–31,120–145] and organic thermoelectric materials,[32,146–157] as well as the emerging MHPs.[21,22,51,54,67,74,158–162] The gray dashed line represents the theoretical *ZT* range of MHPs,[33–36] and the gray dashed box in the bottom right corner indicates the experimental values obtained for MHPs. (B) Schematic illustration showcasing the advantages of MHPs for thermoelectrics. (C) Prospect of optimizing *ZT* through carrier concentration tuning via doping from the current status to the ideal range, highlighting the needs for effective doping methods. (D) Key conceptual development stages of conventional inorganic thermoelectric materials, with MHPs in the early stages of research requiring investigation into electrical doping strategies.

limited by their relatively low mobility, limiting their efficiency as thermoelectric generators. On the other hand, MHPs offer a promising alternative for thermoelectric applications due to their unique properties, combining the high mobility[24] of inorganic materials with the ultralow thermal conductivity[19–21] and facile processing[4,10,11,14] of organic materials (see Figure 1B), making them a strong candidate for next-generation thermoelectric materials supported by various theoretical predictions.[33–36]

However, the low electrical conductivity, and therefore a low power factor, of MHPs has been one of the main limiting factors for realizing high thermoelectric figure of merit (*ZT*), unlike numerous theoretical results previously reported in the field,[33–36] mainly due to the absence of effective doping methods for controlling their carrier concentration (see Figure 1A,C). Previous doping studies in MHPs have mainly focused on improving their optical properties or film quality and stability, whereas tackling the inherent electrical doping issues in MHPs has not been particularly emphasized.[37–40]

In this critical review, we attempt to address the importance of developing effective doping strategies for MHP thermoelectrics and the resulting impact on charge transport mechanisms. While previous reviews have mainly focused on the general thermoelectric[41,42] and thermal transport properties[43,44] of MHPs, a gap remains in directly addressing electrical doping strategies[45–48] for MHP thermoelectrics and their resulting impact on charge transport. To fill this gap, we first discuss three types of electrical doping methods implemented in MHPs and recent studies on doping-enhanced thermoelectric performance of MHPs. Subsequently, we provide insights into the charge transport mechanism under the influence of electron–phonon coupling in MHPs and discuss different models proposed. Finally, we address main doping challenges both at mechanistic, materials- and device-level for advancing the field of MHP thermoelectrics, followed by research visions for potential breakthroughs in the field.

2 | ELECTRICAL DOPING IN MHP THERMOELECTRICS

The thermoelectric performance of a material is quantified using the dimensionless figure of merit, *ZT*.[49] A high *ZT* value indicates that a material is more efficient at converting heat into electricity. *ZT* is defined by the following equation:

$$ZT = \frac{\sigma S^2}{\kappa} T \tag{1}$$

where S is the Seebeck coefficient, σ is the electrical conductivity, κ is the thermal conductivity, and T is the absolute temperature. Therefore, in the case of conventional inorganic thermoelectric materials, breakthroughs in *ZT* values have been achieved by first optimizing the electrical doping range, which is directly related to electrical conductivity, then minimizing thermal conductivity through nanostructuring, and finally enhancing the Seebeck coefficient using band engineering (see Figure 1D). This also indicates that MHPs, which possess promising properties as thermoelectric materials, are currently at the stage of developing an appropriate electrical doping method, which is considered the first step out of the key historical developments of conventional thermoelectrics. In one theoretical study by Filippetti et al.,[34] the *ZT* value reached its peak with a value between 1 and 2 at the carrier concentration of 10^{19} cm^{-3} and a temperature of 300 K, while the experimental values appear significantly lower in contrast (see Table S1 in the Supporting Information for a summary of the enhanced thermoelectric performance achieved through current doping methods). If effective doping techniques emerge, as in the case of organic thermoelectrics ($ZT > 0.4$),[32] MHPs with their generally favorable crystalline structures for charge transport could potentially achieve higher *ZT* values than organic thermoelectric materials. In this section, we discuss electrical doping methods and dopants that have been applied to MHPs, focusing on their impact on thermoelectric properties. Electrical doping methods for MHPs can be categorized into three main types (see Figure 2A–C), based on the mechanism for generating excess charge carriers within the MHP crystal structure and the location of dopants: intrinsic defect doping (self-doping), extrinsic defect doping (substitutional doping and interstitial doping), and charge transfer doping (molecular doping).

2.1 | Intrinsic defect doping

The most common method for increasing charge concentration in MHP thermoelectrics is through intrinsic defect doping, also known as self-doping. As shown in Figure 2A, the self-doping originates from the formation of charged intrinsic defects, such as vacancies or interstitials within the ABX_3 structure,[45] which can generate excess charge carriers, and thereby enhance electrical conductivity. For example, Sn-based MHPs are prevalent as thermoelectric materials because they can achieve higher electrical conductivity compared to Pb counterparts (see Figure S1 in the Supporting Information), mainly due to the facile p-type doping introduced by Sn^{2+} oxidation[50]:

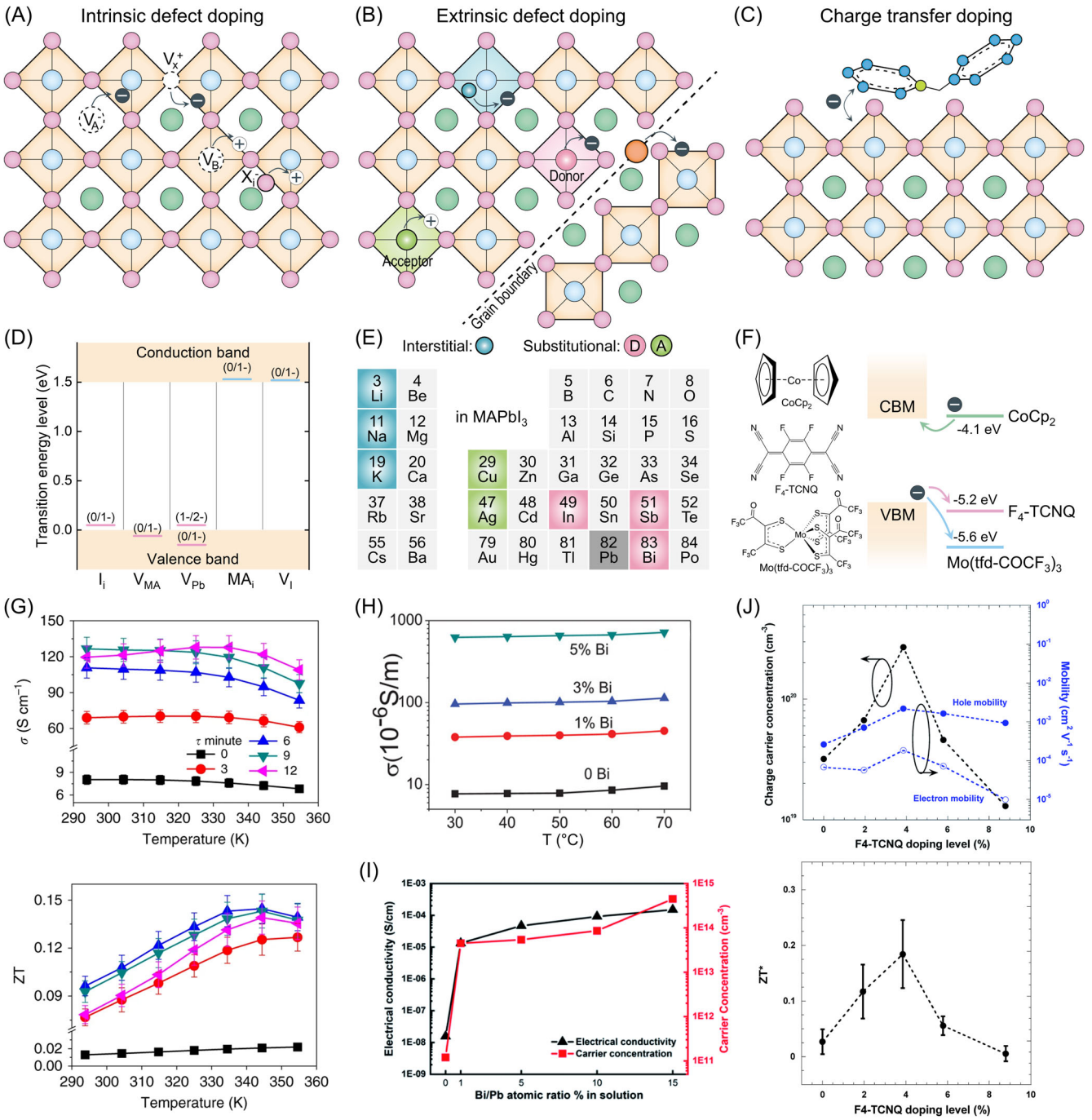

FIGURE 2 (A) Schematic representation of intrinsic defect doping, with vacancies indicated by dashed line circles and halide interstitials, acting as dopants. (B) Schematic of extrinsic defect doping, where the blue and orange atoms acts as n-type dopants at an interstitial site and at grain boundary, respectively. The pink and green atoms represent B-site substitutional dopants, functioning as donors and acceptors, respectively. (C) Schematic of charge transfer doping at the perovskite surface by a molecular dopant. (D) Calculated intrinsic acceptor (pink) and donor (blue) transition energy levels for $MAPbI_3$. Adapted with permission.[60] Copyright 2014, AIP Publishing. (E) Truncated periodic table of elements summarizing dopants that commonly function as interstitial (blue) and B-site substitutional donors (pink) and acceptors (green) in $MAPbI_3$. (F) HOMO and LUMO of representative n-type and p-type molecular dopants. (G) Temperature dependence of electrical conductivity (top) and *ZT* (below), with differently colored curves representing varying degrees of oxidation. Reproduced with permission.[51] Copyright 2019, Springer Nature. (H) Electrical conductivity at different temperatures for undoped and Bi-doped $MAPbBr_3$ thin films. Reproduced with permission.[66] Copyright 2019, John Wiley and Sons. (I) Electrical conductivity and number of charge carriers for Bi-doped $MAPbBr_3$ single crystals. Reproduced with permission.[67] Copyright 2020, Royal Society of Chemistry. (J) Charge carrier concentration, electron and hole mobilities (top) and *ZT* values (bottom) of F_4-TCNQ doped $FASnI_3$ thin films as a function of doping level. Reproduced with permission.[74] Copyright 2020, Royal Society of Chemistry.

$$\mathrm{Sn_{Sn}(II)} + \mathrm{O_2} \rightarrow \mathrm{V_{Sn}^0} + \mathrm{Sn(IV)O_2} + 2\mathrm{h}^+ \rightarrow \mathrm{V_{Sn}^{2-}} + 4\mathrm{h}^+ + \mathrm{Sn(IV)O_2} \quad (2)$$

The heavy p-type doping in Sn-based MHPs results from the lower redox potential of the Sn^{2+}/Sn^{4+} pair (+0.15 V) compared to the Pb^{2+}/Pb^{4+} pair (+1.67 V) in Pb-based MHPs.[50] To adjust the electrical conductivity of Sn-based MHPs through self-doping, the degree of oxidation is tuned primarily by varying the air exposure time (see the top figure of Figure 2G). In a study by Liu et al.,[51] the electrical conductivity of $CsSnI_3$ films was increased through Sn-based self-doping, while ambient stability was improved using a $SnCl_2$ surface protection layer. By optimizing self-doping in the $SnCl_2$ surface protection layer, which was deposited by seed layer plus sequential deposition method, they enhanced the thermoelectric performance of the underlying $CsSnI_3$ film as it gained free charges from the $SnCl_2$ layer, ultimately achieving ZT of 0.14 at room temperature (see the bottom figure of Figure 2G). This approach effectively doped the active $CsSnI_3$ layer in bulk while minimizing dopant-induced scattering, similar to modulation doping,[52,53] due to the physical separation between the doped layer (i.e., $SnCl_2$) and the channel ($CsSnI_3$). While this approach effectively raises the electrical conductivity of Sn-based MHPs, it also leads to degradation due to oxidation, making it crucial to develop doping techniques that ensure both tunability in conductivity and material stability. Qian et al.[54] demonstrated the enhancement of stability in Sn self-doped samples by synthesizing $CsSn_{1-x}Ge_xI_3$ through solid-state sintering, achieving a ZT of 0.123 at 473 K and approximately 0.09 at room temperature. This work was based on a previous report in which the alloying of Sn with Ge in $CsSnI_3$ was systematically investigated for enhancing the ambient stability of MHP-based solar cells.[55] More specifically, it was confirmed by x-ray diffraction (XRD) analysis that in the case of $CsSnI_3$, 89% of it degraded into the non-perovskite phases, δ-$CsSnI_3$ and Cs_2SnI_6, after 5 h in ambient conditions with a high relative humidity of ∼65% whereas $CsSn_{0.8}Ge_{0.2}I_3$ experienced only 33% degradation after 5 h. Overall, this finding suggests that the stability improvement strategies developed for solar cells and other optoelectronic devices, where MHPs have been actively studied, can also be effectively applied to thermoelectrics.

Similar intrinsic defect doping approaches can be envisaged in Pb-based MHPs, such as methylammonium lead iodide ($MAPbI_3$).[56–59] Many intrinsic defects in $MAPbI_3$ are shallow with respect to the conduction band minimum (CBM) and valence band maximum (VBM), allowing them to act as dopants at room temperature (see Figure 2D).[60] In $MAPbI_3$, the type of carrier is determined by the relative defect density of representative intrinsic defects, such as I vacancy (V_I), MA vacancy (V_{MA}), Pb vacancy (V_{Pb}), and I interstitials (I_i), which can function as p-type or n-type dopants depending on their respective transition energy levels.[60] Although such attempts have been rarely reported in $MAPbI_3$-based thermoelectrics, the defect formation energy in $MAPbI_3$ can be tuned by varying the ratio of MAI and PbI_2 in the precursor,[56] which can be extended to developing intrinsic defect doping methods. Moreover, the different transition energy levels of the existing defects in MHPs with respect to their CBM and VBM also open up routes for adjusting the sign of the Seebeck coefficient in MHPs. Liu et al.[57] reported that it was possible to switch between n-type and p-type conduction in MHPs by creating a $MAPbI_xCl_{3-x}$ with a partial substitution of I with Cl in $MAPbI_3$. This is because the V_{MA}, which can act as a p-type dopant, plays a primary role in single halide $MAPbI_3$, but the introduction of Cl reduces the defect density of V_{MA} and n-type doping becomes dominant.

Unlike in MHP-based solar cells, where preventing the reaction at the interface between the MHP active layer and the electrode is one of the most significant challenges for ensuring device stability,[61] some previous works in MHP thermoelectrics have attempted to utilize this reaction. Wu et al.[58] demonstrated that both p-type and n-type doping could be achieved through the interaction of metal and ion at the metal and $MAPbI_3$ interface. At the Au/$MAPbI_3$ interface, V_{MA} was induced by the interaction between MA^+ and Au atoms, resulting in p-doping, while at the Ag/$MAPbI_3$ interface, the reaction of I^- with Ag contact generated V_I, leading to the formation of an n-doped region. Utilizing this effect, Xie et al.[59] demonstrated a $MAPbI_3$ single-crystal thermoelectric module that employed doping induced by the reaction between $MAPbI_3$ and metal electrodes (Au and Ag). By connecting the $MAPbI_3$ single crystal to the ITO substrate and depositing Au and Ag electrodes to form p-type and n-type legs, respectively, the module generated a thermoelectric voltage of 337 mV at 115°C, with the maximum output power of 30 nW. This study not only aimed to improve the thermoelectric performance of MHPs but also directly demonstrated the potential of MHP as an active material in thermoelectric modules, provided that their electrical conductivity can be increased sufficiently.

2.2 | Extrinsic defect doping

Extrinsic defect doping is a method of introducing impurity atoms into a crystal structure, which results in the formation of extrinsic defect energy levels within

the band gap and the generation of extra charge carriers (see Figure 2B). It is a widely employed type of doping in semiconductor industry, where substitutional doping in high-purity semiconductors has been successfully implemented. However, in the case of MHPs, extrinsic doping by atomic substitution has been challenging due to the soft nature, which makes them prone to forming intrinsic defects that consequently lead to charge compensation.[46]

The possibility of interstitial or substitutional doping generally depends on the ionic radius of the dopant, with smaller ionic radius dopants tending to occupy interstitial sites and those with an ionic radius similar to MHP constituent elements (mostly B-site elements for electrical doping, see Figure 2E) favoring substitutional sites, and this relationship can be predicted using the Goldschmidt tolerance factor.[62] However, not only the ionic radius but also factors such as dopant concentration and doping method can influence the doping type and efficiency.[63–65] For example, Ag can act as a p-type dopant when substituting the Pb site in $MAPbI_3$,[63,64] but they can also function as an effective n-type dopant when segregated on the surface, enabling metallic transport.[65]

Extrinsic doping of MHPs for thermoelectrics has been rarely reported, except for a few reports on Bi doping.[66,67] These studies all used Bi as an impurity dopant, but they reported distinct doping effects, illustrating that the impact of Bi doping varies depending on its location. Xiong et al.[66] fabricated devices by mixing BiI_3 into a $MAPbI_3$ solution precursor and spin-coating the mixture, finding that Bi dopants were present not only within the grains but also at the grain boundaries. Bi-rich grain boundaries were found to form charge transport channels, which reduced the V_{Pb} concentration and trap density, consequently enhancing mobility. In the 5% Bi-doped film, the electrical conductivity increased by more than two orders of magnitude (see Figure 2H), and the power factor at 70°C increased by three orders of magnitude to 3.8×10^{-6} μW mK^{-2} compared to the pristine film, albeit with the power factor being significantly lower than the Sn counterpart. On the other hand, Tang et al.[67] synthesized single crystals by substituting Bi dopants into the Pb site using an inverse temperature crystallization method, and in 15% Bi-doped $MAPb_{1-x}Bi_xBr_3$, they confirmed n-type doping through a negative Seebeck coefficient of −378 μV K^{-1}, while observing a four-order increase in the carrier concentration (see Figure 2I). Overall, the above studies highlight the need for an effective doping strategy that considers multiple factors, such as the doping method to enhance the incorporation of dopants within the perovskite lattice, and dopant-MHP material selection rules based on a mechanistic understanding of extrinsic defect doping, particularly the exact doping sites (i.e., interstitials or substitutional sites within the lattice or grain boundaries).

2.3 | Charge transfer doping

Charge transfer doping refers to the doping process that occurs through charge transfer between a host semiconductor and a molecular dopant (see Figure 2C).[68,69] The molecular dopants act as either donors or acceptors based on their relative energy levels, where donating electrons to the host is energetically favorable when their highest occupied molecular orbital (HOMO) is above the CBM of the MHP (i.e., n-type doping) and accepting electrons from the host when their lowest unoccupied molecular orbital (LUMO) is below the VBM of the MHP (i.e., p-type doping), as shown in Figure 2F. In MHPs, various molecular dopants have been employed for molecular doping, such as 2,3,5,6-tetrafluoro-7,7,8,8-tetracyanoquinodimethane (F_4-TCNQ)[70,71] and molybdenum tris-(1-(trifluoroacetyl)-2-(trifluoromethyl)ethane-1,2-dithiolene) (Mo(tfd-$COCF_3)_3$),[72] which are strong molecular acceptors (p-type dopants), and a strong molecular donor (n-type dopant) bis(cyclopentadienyl)cobalt(II) ($CoCp_2$).[73] Most of the previous reports in MHPs have focused on surface charge transfer doping of MHP films for enhancing extraction of photogenerated carriers in solar cells[70,72] and photodetectors.[73] However, there has been only limited research on utilizing molecular doping in MHP thermoelectrics. One notable example is a study by Zheng et al.,[74] in which doping formamidinium tin iodide ($FASnI_3$) thin film with F_4-TCNQ showed a markedly improved *ZT* value of 0.19 at room temperature from 0.03 in its pristine state. It was reported that F_4-TCNQ doping not only improved the charge carrier concentration of the $FASnI_3$ thin film but also enhanced the mobility by affecting the film morphology (i.e., reducing pinholes and larger grain sizes), enabling better charge transport (see Figure 2J).

While molecular charge transfer doping has been employed in MHPs based on the aforementioned energetics criteria,[48] it is not the sole parameter in consideration. Especially for MHPs, molecular dopants have been shown to dope host materials by residing at grain boundaries or surfaces, rather than entering the crystal structures of the host material,[45,48] which limits the charge transfer processes to the exteriors of grains. This is mainly due to the size of dopant molecules, which are typically too large to diffuse into the bulk of MHP films. This makes it challenging to achieve effective bulk doping challenging and limits the doping range, unlike conventional doping in inorganic semiconductors. In addition, while their doping mechanisms, such as ion-pair formation or charge

transfer complex formation,[68,69] are relatively well understood in organic semiconductors, the mechanisms by which molecular dopants dope MHP host materials have not yet been elucidated. Some studies have reported that molecular dopants can also induce morphological changes in MHPs,[48] highlighting the importance of conducting further studies that can reveal the doping mechanism via a quantitative and systematic assessment of the doping efficiency, and the resulting charge transport mechanism, inclusive of the doping-induced structural changes.

3 | CHARGE TRANSPORT MECHANISM IN MHPS FOR THERMOELECTRICS

Understanding the charge transport mechanism of MHPs is vital for optimizing thermoelectric performance, as the figure of merit, *ZT*, directly depends on transport properties. Particularly, since mobility is proportionally related to electrical conductivity, examining the charge transport mechanism of doped MHPs is as crucial for thermoelectric devices as developing efficient doping for MHPs. In MHPs, the charge transport mechanism is shown to be heavily influenced by lattice interactions (i.e., electron–phonon coupling). The significant degree of electron–phonon coupling in MHPs leads to the formation of polarons, which are quasiparticles that form when an electron or hole interacts with a polarization field, causing the carrier to become localized while being surrounded by a cloud of phonons.[75–77] The formation of polarons and the presence of dynamic disorder in MHPs are considered responsible for the discrepancy between the theoretical predictions of up to the order of 1000 $cm^2 V^{-1} s^{-1}$ and empirical values (up to approximately 100 $cm^2 V^{-1} s^{-1}$).[20,24,78,79] In MHPs, both small and large polarons are known to exist (see Figure 3A).[75,76,80,81] Small polarons are charge states strongly associated with local structural distortion and are induced by self-trapping of an electron or hole in the crystal lattice due to its interaction with lattice vibrations, resulting in incoherent hopping transport, whereas large polarons are relatively delocalized and exhibit more coherent band-like transport. In the field, both small and large polarons in MHPs have been explored using spectroscopic analysis and theoretical modeling methods. Neukirch et al.[82] provided theoretical evidence of polaron formation in $MAPbI_3$ using density functional theory (DFT) calculations, from which small polarons in $MAPbI_3$ could be linked to the reorientation of MA^+ molecular dipoles and volumetric lattice strain (see Figure 3B). Experimental results obtained through femtosecond impulsive stimulated Raman spectroscopy by Park et al.[83] supported this claim, demonstrating that the formation of small polarons in $MAPbI_3$ is associated with structural distortion of the inorganic Pb-I framework. Large polaron formation has also been investigated by Miyata et al.,[81] examining $MAPbBr_3$ and $CsPbBr_3$ single crystals using time-resolved optical Kerr effect spectroscopy, which showed that the $PbBr^{3-}$ sublattice deformation is primarily responsible for large polaron formation in both crystals (see Figure 3C). Theoretical research by Zheng et al.[84] used a tight-binding model based on DFT calculations to study large polaron formation in $MAPbI_3$ and its impact on charge transport, demonstrating how dynamic disorder and large polaron effects influence the electronic structure and carrier dynamics.

The above studies on polaron formation in MHPs have mainly focused on pristine MHPs without considering electrical doping. The effects of electron–phonon coupling are expected to be critical in determining charge transport, especially in doped MHPs, which are highly relevant for thermoelectrics and become more complex in the presence of impurity atoms for extrinsically doped MHPs. Impurity atoms, used as dopants in extrinsic defect doping, can greatly impact the local electronic environment depending on whether they occupy either interstitial or substitutional sites in the crystal lattice.[78,82,85] In the case of substitutional doping, the dopant directly replaces an atom in the lattice, leading to changes in the local bonding environment, which can substantially impact the formation and characteristics of polarons. Therefore, it is crucial to carefully consider these effects when investigating charge transport in MHPs doped by extrinsic defect doping.

Temperature dependence measurements have been a powerful probe for investigating and distinguishing the underlying charge transport models in disordered semiconductors.[86–88] In MHPs, numerous studies have reported a negative slope in the mobility versus temperature behavior, indicating that phonon effects contribute significantly to charge transport.[89–91] The charge transport models employed to account for the exact temperature dependence in MHPs discuss two possible mechanisms: acoustic deformation potential (ADP) scattering and Fröhlich interactions. While some experimental studies have suggested a $T^{-1.5}$ dependence of mobility (see Figure 3D),[89–91] indicating the possible importance of scattering by ADP, numerous reports highlight the role of multiple phonon modes and strong phonon anharmonicity in materials like $MAPbI_3$, which can be better described with Fröhlich-type polar interactions.[75] Due to the ionic character of MHPs, the contribution of Fröhlich-type polar interactions, which occur when the polarization of the ionic lattices creates electric fields that interact with the electrons in the system, is expected to be dominant, as suggested by several studies.[81,84,92–94]

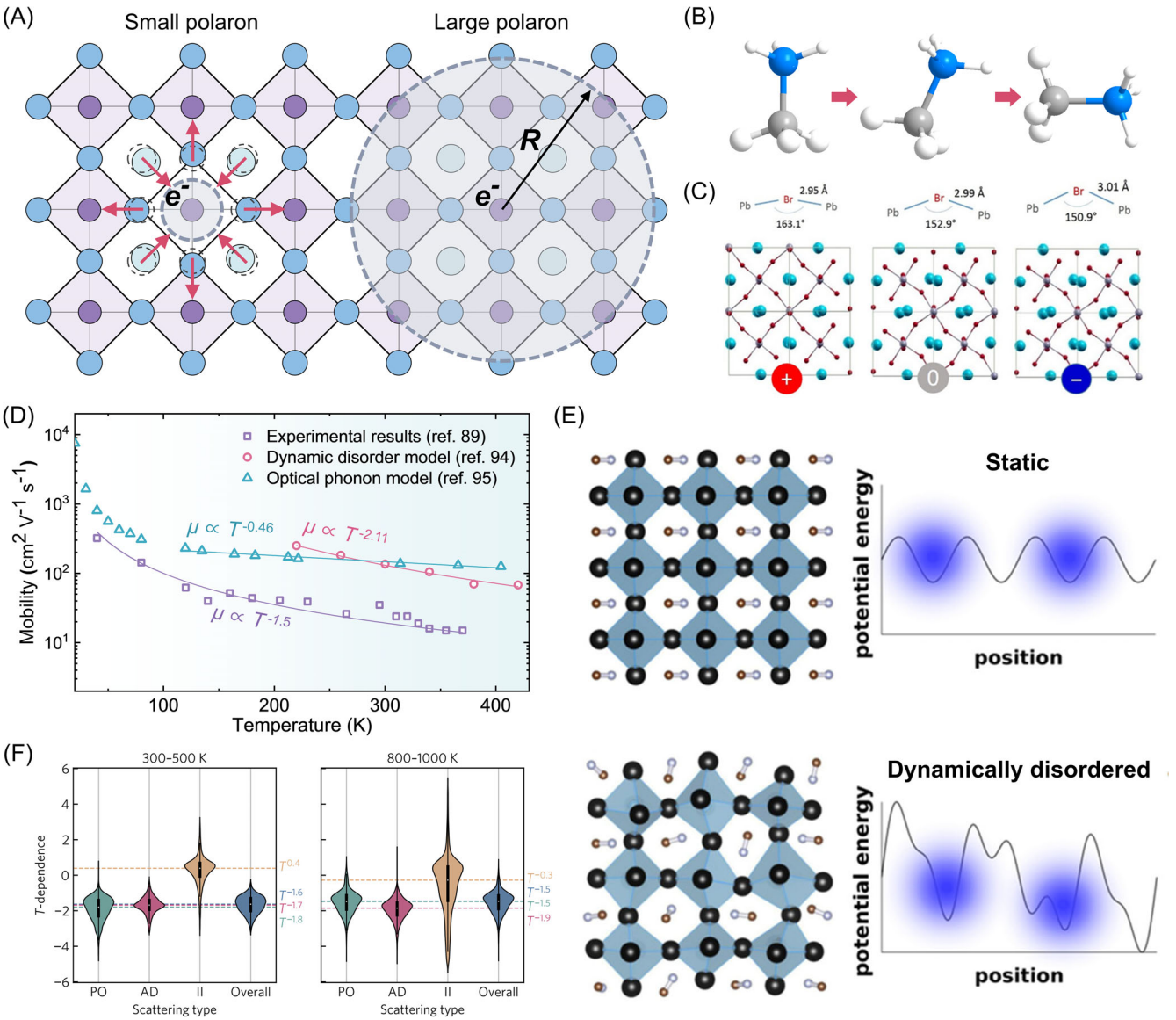

FIGURE 3 (A) Schematic of small (left) and large (right) polarons in 3D MHPs. (B) Rotational motion of the MA molecule. (C) Changes in Pb-Br-Pb bending and Pb-Br bond length with relaxed structures of $MAPbBr_3$ upon positive (left) and negative (right) charge injection. Reproduced with permission.[81] Copyright 2017, American Association for the Advancement of Science. (D) Experimental[89] and theoretical[94,95] temperature-dependent mobility plot of $MAPbI_3$ Reproduced with permission.[89] Copyright 2015, John Wiley and Sons. Reproduced with permission.[94] Copyright 2017, American Physical Society. Reproduced with permission.[95] Copyright 2018, American Chemical Society. (E) Schematic illustration of dynamic disorder in MHPs. In the static scenario (top), a perfectly periodic lattice leads to a periodic energy landscape, whereas in the dynamic disorder scenario (bottom), fluctuations in the potential landscape induced by lattice dynamics that transiently localize charges. Reproduced with permission.[78] Copyright 2021, American Chemical Society. (F) Temperature-dependent mobility for different scattering mechanisms. Histograms represent low temperature range 300–500 K (left) and high temperature range 800–1000 K (right), obtained from 23 000 materials. Calculations were performed using the AMSET package at a carrier concentration of 10^{17} cm^{-3} and are categorized into polar optical (PO), acoustic deformation potential (AD), and ionized impurity (II) scattering.[88] Reproduced with permission from arXiv under the CC BY 4.0 License.

This happens through the creation of an electric field by longitudinal optical (LO) phonon modes, resulting in polarization. While the Fröhlich interaction-based model effectively predicts the mobility of MHPs at room temperature, it has limitations in accurately predicting the temperature-dependence of mobility. The model estimates the temperature dependence of polaron mobility to be around $T^{-0.5}$ (see Figure 3D),[94] differing from the $T^{-1.5}$ observed in experimental results.[89] Although a complete mechanism requires further investigation, this

discrepancy can be attributed to carrier localization due to dynamic disorder (see Figure 3E). The dynamic disorder model can be employed to describe transiently localized charge carriers resulting from a slowly evolving electrostatic potential landscape driven by soft and anharmonic lattice dynamics in MHPs and is known to predict a $T^{-2.11}$ dependence of mobility (see Figure 3D).[95]

Although the above polaron formation and transport models provide valuable insights into the charge transport of MHPs, a recent theoretical study has highlighted that even within the same scattering mechanism, there exists a finite variation in the temperature dependence of mobility depending on the constituent elements (i.e., optical phonon mode), band structure (e.g., non-parabolic bands), temperature range and doping levels (see Figure 3F).[88] Therefore, a more sophisticated model is needed for examining the charge transport in MHPs, especially when additional factors such as ionic effects and microstructural aspects are considered important. Incorporating all these factors into a single model is challenging, but they are still highly relevant for the performance of thermoelectric devices.

4 | DOPING CHALLENGES FOR ADVANCING MHP THERMOELECTRICS

4.1 | Mechanistic understanding of electrical doping

A more comprehensive phenomenological understanding of the excess carrier generation mechanism for each doping method in MHPs should be developed. This requires in-depth quantitative and systematic analyses of each doping process to extract doping efficiency (i.e., the number of free carriers generated per dopant) and to figure out key selection criteria for appropriate dopants. This requires understanding the energetics related to the formation of dopant levels and their relative position with respect to CBM or VBM to assess the probability of their charging via thermal excitation both from theoretical and experimental studies. In addition to the simple energetics requirements, accurately identifying the doping sites within MHPs (i.e., substitutional or interstitial sites within the lattice or grain boundaries) will contribute to developing multi-scale structure–property relationships for electrical doping in MHPs. Since we expect a heavy doping regime is relevant for optimizing the thermoelectric performance of MHPs, which has rarely been discussed in the field, the level of structural disorder induced by the high dopant loading is expected to be critical in determining the free carrier generation.

4.2 | Understanding charge transport at heavy-doping-regime

In addition to the doping mechanism that accounts for the free carrier generation, doping is only meaningful when the generated carriers can undergo efficient charge transport in MHPs. Therefore, understanding doping effects on charge transport at the heavy-doping-regime is an essential milestone for advancing MHP thermoelectrics. In our review, we dealt in depth with the role of electron–phonon coupling in charge transport mechanisms in MHPs. In the heavy-doping-regime, carrier scattering by dopant impurities (e.g., dopant counterions or Sn^{4+} impurities) is expected to be significant or even comparable, which complicates the transport model to incorporate the Coulomb potential landscapes formed by these impurities (see Figure 4). This is interrelated to constructing the aforementioned multi-scale structure–property relationships, which have been underdeveloped for understanding both doping and transport processes at high doping levels. Specifically, the location and the spatial distribution of dopants within MHPs can affect the MHP crystal structure (e.g., microstrain effects[96]) or microstructure (e.g., dopants concentrated at grain boundaries[97,98]) and dictate the energetic disorder in the electronic structure and the charge transport limited by charged impurity scattering, which adds to the complexity of the charge transport mechanism in MHPs in the presence of intrinsic defects, grain boundaries, and compositional inhomogeneity.[99]

4.3 | Developing non-invasive bulk doping strategies

The dopant selection criteria obtained from the above mechanistic understanding can guide us toward constructing perovskite-dopant combinations and envisaging doping strategies that can be (1) efficient (i.e., generating many free carriers per dopant), (2) controllable (over a wide range of carrier concentrations), and (3) preserving the intrinsic charge transport properties (i.e., non-invasive). The widely-used Sn self-doping strategy in Sn-based MHPs, on the other hand, can effectively improve electrical conductivity but compromises the composition, structure, and device stability of materials.[50,100] Therefore, it is necessary to explore doping strategies that utilize dopants capable of controlling the electrical conductivity over a wide range without adversely affecting other properties by minimizing the structural degradation and disorder. This leads to the necessity of bulk doping, for which many challenges remain in bulk-incorporating dopants in the perovskite structure, especially molecular dopants

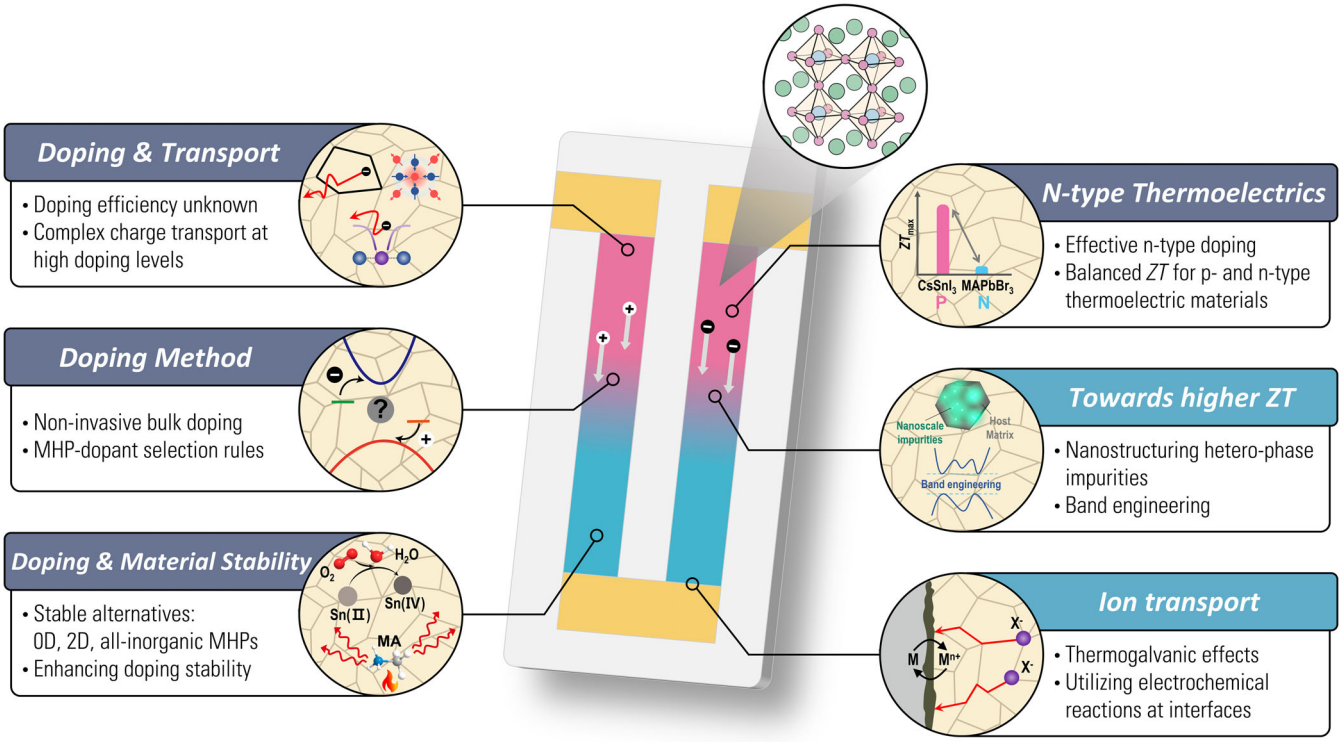

FIGURE 4 Schematic illustration depicting the challenges (dark gray) and new opportunities (blue) of MHP thermoelectrics.

for charge transfer doping which are often too large to penetrate into the bulk. To achieve this, effective doping methods that take advantage of intrinsic structural features could be envisaged, such as implementing bulk doping by inserting molecular dopants into the "non-active" organic spacer layer of 2D RP structures[101] or utilizing grain boundaries as paths for diffusing dopants in MHP films.

4.4 | N-type thermoelectrics

The current records for n-type MHP thermoelectrics fall significantly below that of p-type in terms of *ZT*, despite many theoretical predictions favoring the thermoelectric performance of n-type over p-type due to the band anisotropy of CBM,[34] which increases the power factor[28,102,103] and a lower effective mass of electrons predicted from DFT calculations[36] that guarantee excellent charge transport properties. One of the main reasons is the insufficient number of free carriers available for electrical conduction in n-type MHPs due to the lack of effective n-type doping methods compared to, for example, p-type doping by self-doping for Sn-based MHPs. Recently, Lin et al.[65] reported successfully implementing n-type doping in $MAPbI_3$ using metal halide dopants, which led to a 3–4 order of magnitude increase in the dark current of $MAPbI_3$ thin films. However, while this level of conductivity is quite high among n-type $MAPbI_3$, it is still lower than 14 S cm^{-1} observed in Sn-based MHPs,[74] for which one of the highest *ZT* values among MHPs to date was reported. In order to develop all-MHP-based thermoelectric generators, it is crucial to conduct studies on n-type doping, as having balanced *ZT* values between p- and n-type MHPs is essential for constructing efficient thermoelectric generators.

4.5 | Material and doping stability

While MHPs are primarily intended for use in low-temperature thermoelectric devices operating near room temperature, ensuring both ambient and thermal stability of MHPs is a crucial challenge, especially for Sn-based MHPs, which have demonstrated the best thermoelectric performance to date but are susceptible to degradation due to ready oxidation.[104] Sn vacancy-induced self-doping in Sn-based MHPs leads to thermoelectric performances that are notably higher compared to Pb-based MHPs, underscoring the need for the development of other doping methods (see Figure S1 in the Supporting Information). To achieve long-term material and doping stability, more stable alternatives can be explored, such as Pb-based MHPs, low-dimensional MHPs like 2D or 0D

structures, and all-inorganic MHPs (i.e., not containing volatile organic cations). Recent studies have also indicated that double perovskites and other low-dimensional MHPs could offer higher stability while possessing desirable thermoelectric properties (low κ and high S),[36,105–108] such as Cs_2AgBiX_6,[105] Cs_2AgInX_6,[106] $Cs_3Cu_2I_5$,[36] and some 2D MHPs.[107,108] Here, the main challenge is, again, inventing suitable doping methods to increase their doping levels. Doping stability is crucial for thermoelectrics, as the high doping levels required may cause significant structural changes and even damage in some cases.[73] In molecular doping using strong reducing or oxidizing agents as potential candidates for high doping levels, chemical damage may occur in defect-prone MHPs when they bond with uncoordinated metal cations, subsequently releasing halide ions.[73] Therefore, extra caution is required for establishing dopant selection rules by considering potential structural and chemical damages upon doping.

5 | FUTURE PROSPECTS: BEYOND DOPING AND UNIQUE PROPERTIES

Although this review has mainly dealt with the electrical doping perspectives for MHP thermoelectrics, there exists ample room for exploring opportunities beyond doping and adopting compelling methodologies such as nanostructuring[109] and band engineering,[110] which have been key developments in conventional high-thermoelectric-performance materials. Nanostructuring MHPs (with intrinsically low thermal conductivity) has the prospect of further inducing phonon-scattering by forming nanostructured phases within the bulk material.[103] In MHPs, hetero-phase impurities have been studied for light emitters, where luminescent nano-sized 3D phase particles were endotaxially grown within a bulk 0D matrix.[14] They have also been explored for steering charge transport paths in MHP-based LEDs.[111] Both applications may be relevant, but proper band alignment at the interfaces is crucial to ensure effective charge transport paths in the bulk. Additionally, a band engineering approach can be proposed to maximize anisotropy in band dispersion (i.e., anisotropic effective masses) and achieve multi-band convergence for accessing multi-band transport via degeneracy at band extrema, which has rarely been discussed in MHPs. Therefore, while the current research priority for MHP thermoelectrics should remain on increasing power factor through effective doping methods, combining these strategies with nanostructuring and band engineering could potentially lead to significant improvements in their thermoelectric performance.

The thermoelectric potential of MHPs is not limited to the ultimate goal of constructing highly efficient thermoelectric generators but can be extended to maximize their unique material properties. Notably, the ease of halide ion migration[112,113] is both a challenge and a new avenue for opportunities. Halide ions can actively participate in redox reactions at the interface with the metal electrode, resulting in electrochemical reactions at the electrode/channel interfaces,[114] which can significantly impact both the stability and performance of thermoelectric devices. However, we propose that this property can be harnessed to generate electrical power via the thermogalvanic effect,[115] in which the migration of mobile halide ions can create an electrochemical potential difference when subjected to a temperature gradient, subsequently generating electrical power, if properly controlled. Exploiting the thermogalvanic effect in MHPs could open new routes as a low-cost material for solid-state thermogalvanic energy conversion. In addition, their superior optoelectronic properties, including high absorption coefficient, slow hot-carrier cooling,[116] and long carrier lifetime[117] can offer a unique physical basis for the unexplored area of photo-thermoelectric effects,[118,119] and designing photovoltaic-thermoelectric hybrid devices where the waste heat from solar power conversion can be harnessed as a useful form of electrical energy, increasing the overall solar energy conversion efficiency.

Overall, our critical assessment of electrical doping for MHP thermoelectrics signifies the remaining challenges and opportunities in the field for better understanding doping effects on charge transport and developing effective doping methods. While potential solutions can be inspired by the well-established field of MHP optoelectronics, the required materials and dopant selection rules are expected to differ significantly for doping levels of interests in thermoelectrics, mostly marking unexplored regimes of doping and transport in MHPs. Therefore, in addition to the main quest for improving the ZT of the promising material systems, future research on thermoelectric properties of doped MHPs can reveal rich underlying charge transport physics in the presence of charged impurities. Despite the remaining challenges, this review promotes the promising prospects of MHPs for thermoelectrics owing to their distinctive material properties which can be synergistically utilized with the existing key concepts in the field of conventional thermoelectrics that can include, or go beyond nanostructuring and band engineering.

AUTHOR CONTRIBUTIONS

Yongjin Kim: Conceptualization, writing - original draft, visualization (figure creation), analysis, and data curation; **Hyeonmin Choi:** Conceptualization, visualization, and

data curation; **Jonghoon Lee:** Data curation and writing - original draft; **Young-Kwang Jung, Joonha Jung, and Jaeyoon Cho:** Data curation; **Takhee Lee:** Writing - review & editing and supervision; **Keehoon Kang:** Conceptualization, validation, writing - review & editing, and supervision.

ACKNOWLEDGMENTS

This work was supported by the New Faculty Startup Fund from Seoul National University. The authors appreciate the financial support of the National Research Foundation of Korea (NRF) grant (No. 2021R1C1C1010266 and No. 2021R1A2C3004783), the BrainLink Program (No. 2022H1D3A3A01077343), and the Nano Material Technology Development Program grant (No. 2021M3H4A1A02049651) through NRF funded by the Ministry of Science and ICT (MSIT) of Korea.

CONFLICT OF INTEREST STATEMENT

The authors declare no conflict of interest.

ORCID

Yongjin Kim https://orcid.org/0009-0003-9580-9258
Keehoon Kang https://orcid.org/0000-0003-1230-3626

REFERENCES

1. Park J, Kim J, Yun HS, et al. Controlled growth of perovskite layers with volatile alkylammonium chlorides. *Nature*. 2023;616(7958):724-730. doi:10.1038/s41586-023-05825-y
2. Burschka J, Pellet N, Moon SJ, et al. Sequential deposition as a route to high-performance perovskite-sensitized solar cells. *Nature*. 2013;499(7458):316-319. doi:10.1038/nature12340
3. Yang WS, Noh JH, Jeon NJ, et al. High-performance photovoltaic perovskite layers fabricated through intramolecular exchange. *Science*. 2015;348(6240):1234-1237. doi:10.1126/science.aaa9272
4. Nie W, Tsai H, Asadpour R, et al. High-efficiency solution-processed perovskite solar cells with millimeter-scale grains. *Science*. 2015;347(6221):522-525. doi:10.1126/science.aaa0472
5. Tan ZK, Moghaddam RS, Lai ML, et al. Bright light-emitting diodes based on organometal halide perovskite. *Nat Nanotechnol*. 2014;9(9):687-692. doi:10.1038/nnano.2014.149
6. Cho H, Jeong SH, Park MH, et al. Overcoming the electroluminescence efficiency limitations of perovskite light-emitting diodes. *Science*. 2015;350(6265):1222-1225. doi:10.1126/science.aad1818
7. Zhao B, Bai S, Kim V, et al. High-efficiency perovskite–polymer bulk heterostructure light-emitting diodes. *Nat Photonics*. 2018;12(12):783-789. doi:10.1038/s41566-018-0283-4
8. Kim YH, Kim S, Kakekhani A, et al. Comprehensive defect suppression in perovskite nanocrystals for high-efficiency light-emitting diodes. *Nat Photonics*. 2021;15(2):148-155. doi:10.1038/s41566-020-00732-4
9. Hassan Y, Park JH, Crawford ML, et al. Ligand-engineered bandgap stability in mixed-halide perovskite LEDs. *Nature*. 2021;591(7848):72-77. doi:10.1038/s41586-021-03217-8
10. Kim JS, Heo JM, Park GS, et al. Ultra-bright, efficient and stable perovskite light-emitting diodes. *Nature*. 2022;611(7937):688-694. doi:10.1038/s41586-022-05304-w
11. Dou L, Yang Y, You J, et al. Solution-processed hybrid perovskite photodetectors with high detectivity. *Nat Commun*. 2014;5(1):5404. doi:10.1038/ncomms6404
12. Stoumpos CC, Cao DH, Clark DJ, et al. Ruddlesden–popper hybrid lead iodide perovskite 2D homologous semiconductors. *Chem Mater*. 2016;28(8):2852-2867. doi:10.1021/acs.chemmater.6b00847
13. Liang C, Gu H, Xia Y, et al. Two-dimensional Ruddlesden–popper layered perovskite solar cells based on phase-pure thin films. *Nat Energy*. 2021;6(1):38-45. doi:10.1038/s41560-020-00721-5
14. Baek KY, Lee W, Lee J, et al. Mechanochemistry-driven engineering of 0D/3D heterostructure for designing highly luminescent Cs–Pb–Br perovskites. *Nat Commun*. 2022;13(1):4263. doi:10.1038/s41467-022-31924-x
15. Saparov B, Sun JP, Meng W, et al. Thin-film deposition and characterization of a Sn-deficient perovskite derivative Cs2SnI6. *Chem Mater*. 2016;28(7):2315-2322. doi:10.1021/acs.chemmater.6b00433
16. Jun T, Sim K, Iimura S, et al. Lead-free highly efficient blue-emitting Cs3Cu2I5 with 0D electronic structure. *Adv Mater*. 2018;30(43):1804547. doi:10.1002/adma.201804547
17. Saparov B, Mitzi DB. Organic–inorganic perovskites: structural versatility for functional materials design. *Chem Rev*. 2016;116(7):4558-4596. doi:10.1021/acs.chemrev.5b00715
18. Lin H, Zhou C, Tian Y, Siegrist T, Ma B. Low-dimensional organometal halide perovskites. *ACS Energy Lett*. 2018;3(1):54-62. doi:10.1021/acsenergylett.7b00926
19. Pisoni A, Jaćimović J, Barišić OS, et al. Ultra-low thermal conductivity in organic–inorganic hybrid perovskite CH3NH3PbI3. *J Phys Chem Lett*. 2014;5(14):2488-2492. doi:10.1021/jz5012109
20. He Y, Galli G. Perovskites for solar thermoelectric applications: a first principle study of CH3NH3AI3 (A = Pb and Sn). *Chem Mater*. 2014;26(18):5394-5400. doi:10.1021/cm5026766
21. Lee W, Li H, Wong AB, et al. Ultralow thermal conductivity in all-inorganic halide perovskites. *Proc Natl Acad Sci*. 2017;114(33):8693-8697. doi:10.1073/pnas.1711744114
22. Xie H, Hao S, Bao J, et al. All-inorganic halide perovskites as potential thermoelectric materials: dynamic cation off-centering induces ultralow thermal conductivity. *J Am Chem Soc*. 2020;142(20):9553-9563. doi:10.1021/jacs.0c03427
23. Miyata K, Atallah TL, Zhu XY. Lead halide perovskites: crystal-liquid duality, phonon glass electron crystals, and large polaron formation. *Sci Adv*. 2017;3(10):e1701469. doi:10.1126/sciadv.1701469
24. Herz LM. Charge-carrier mobilities in metal halide perovskites: fundamental mechanisms and limits. *ACS Energy Lett*. 2017;2(7):1539-1548. doi:10.1021/acsenergylett.7b00276
25. Jia Y, Jiang Q, Sun H, et al. Wearable thermoelectric materials and devices for self-powered electronic systems. *Adv Mater*. 2021;33(42):2102990. doi:10.1002/adma.202102990
26. Liu R, Wang ZL, Fukuda K, Someya T. Flexible self-charging power sources. *Nat Rev Mater*. 2022;7(11):870-886. doi:10.1038/s41578-022-00441-0
27. Poudel B, Hao Q, Ma Y, et al. High-thermoelectric performance of nanostructured bismuth antimony telluride bulk alloys. *Science*. 2008;320(5876):634-638. doi:10.1126/science.1156446
28. Heremans JP, Jovovic V, Toberer ES, et al. Enhancement of thermoelectric efficiency in PbTe by distortion of the

electronic density of states. *Science*. 2008;321(5888):554-557. doi:10.1126/science.1159725
29. Zhao LD, Lo SH, Zhang Y, et al. Ultralow thermal conductivity and high thermoelectric figure of merit in SnSe crystals. *Nature*. 2014;508(7496):373-377. doi:10.1038/nature13184
30. Shi X, Yang J, Salvador JR, et al. Multiple-filled skutterudites: high thermoelectric figure of merit through separately optimizing electrical and thermal transports. *J Am Chem Soc*. 2011;133(20):7837-7846. doi:10.1021/ja111199y
31. Fu C, Bai S, Liu Y, et al. Realizing high figure of merit in heavy-band p-type half-Heusler thermoelectric materials. *Nat Commun*. 2015;6(1):8144. doi:10.1038/ncomms9144
32. Kim GH, Shao L, Zhang K, Pipe KP. Engineered doping of organic semiconductors for enhanced thermoelectric efficiency. *Nat Mater*. 2013;12(8):719-723. doi:10.1038/nmat3635
33. Lee C, Hong J, Stroppa A, Whangbo MH, Shim JH. Organic–inorganic hybrid perovskites ABI3 (A = CH3NH3, NH2CHNH2; B = Sn, Pb) as potential thermoelectric materials: a density functional evaluation. *RSC Adv*. 2015;5(96):78701-78707. doi:10.1039/C5RA12536G
34. Filippetti A, Caddeo C, Delugas P, Mattoni A. Appealing perspectives of hybrid lead–iodide perovskites as thermoelectric materials. *J Phys Chem C*. 2016;120(50):28472-28479. doi:10.1021/acs.jpcc.6b10278
35. Zhao T, Wang D, Shuai Z. Doping optimization of organic-inorganic hybrid perovskite CH3NH3PbI3 for high thermoelectric efficiency. *Synth Met*. 2017;225:108-114. doi:10.1016/j.synthmet.2017.01.003
36. Jung YK, Han IT, Kim YC, Walsh A. Prediction of high thermoelectric performance in the low-dimensional metal halide Cs3Cu2I5. *NPJ Comput Mater*. 2021;7(1):51. doi:10.1038/s41524-021-00521-9
37. Jin RJ, Lou YH, Wang ZK. Doping strategies for promising organic–inorganic halide perovskites. *Small*. 2023;19(16):2206581. doi:10.1002/smll.202206581
38. Jiang Q, Zhao Y, Zhang X, et al. Surface passivation of perovskite film for efficient solar cells. *Nat Photonics*. 2019;13(7):460-466. doi:10.1038/s41566-019-0398-2
39. Xu L, Yuan S, Zeng H, Song J. A comprehensive review of doping in perovskite nanocrystals/quantum dots: evolution of structure, electronics, optics, and light-emitting diodes. *Mater Today Nano*. 2019;6:100036. doi:10.1016/j.mtnano.2019.100036
40. Shen X, Kang K, Yu Z, et al. Passivation strategies for mitigating defect challenges in halide perovskite light-emitting diodes. *Joule*. 2023;7(2):272-308. doi:10.1016/j.joule.2023.01.008
41. Hu S, Ren Z, Djurišić AB, Rogach AL. Metal halide perovskites as emerging thermoelectric materials. *ACS Energy Lett*. 2021;6(11):3882-3905. doi:10.1021/acsenergylett.1c02015
42. Zhou Y, Wang J, Luo D, Hu D, Min Y, Xue Q. Recent progress of halide perovskites for thermoelectric application. *Nano Energy*. 2022;94:106949. doi:10.1016/j.nanoen.2022.106949
43. Haque MA, Kee S, Villalva DR, Ong WL, Baran D. Halide perovskites: thermal transport and prospects for thermoelectricity. *Adv Sci*. 2020;7(10):1903389. doi:10.1002/advs.201903389
44. Jung Y, Lee W, Han S, Kim BS, Yoo SJ, Jang H. Thermal transport properties of phonons in halide perovskites. *Adv Mater*. 2022;2204872. Published Online August 29. doi:10.1002/adma.202204872
45. Euvrard J, Yan Y, Mitzi DB. Electrical doping in halide perovskites. *Nat Rev Mater*. 2021;6(6):531-549. doi:10.1038/s41578-021-00286-z
46. Amerling E, Lu H, Larson BW, et al. A multi-dimensional perspective on electronic doping in metal halide perovskites. *ACS Energy Lett*. 2021;6(3):1104-1123. doi:10.1021/acsenergylett.0c02476
47. Haque MA, Rosas Villalva D, Hernandez LH, Tounesi R, Jang S, Baran D. Role of dopants in organic and halide perovskite energy conversion devices. *Chem Mater*. 2021;33(21):8147-8172. doi:10.1021/acs.chemmater.1c01867
48. Zhang F, Smith HL, Kahn A. Molecular dopants: tools to control the electronic structure of metal halide perovskite interfaces. *Appl Phys Rev*. 2021;8(4):041301. doi:10.1063/5.0060129
49. Ioffe AF, Stil'Bans LS, Iordanishvili EK, Stavitskaya TS, Gelbtuch A, Vineyard G. Semiconductor thermoelements and thermoelectric cooling. *Phys Today*. 1959;12(5):42. doi:10.1063/1.3060810
50. Zhou Y, Poli I, Meggiolaro D, De Angelis F, Petrozza A. Defect activity in metal halide perovskites with wide and narrow bandgap. *Nat Rev Mater*. 2021;6(11):986-1002. doi:10.1038/s41578-021-00331-x
51. Liu T, Zhao X, Li J, et al. Enhanced control of self-doping in halide perovskites for improved thermoelectric performance. *Nat Commun*. 2019;10(1):5750. doi:10.1038/s41467-019-13773-3
52. Jang J, Kim JK, Shin J, et al. Reduced dopant-induced scattering in remote charge-transfer-doped MoS2 field-effect transistors. *Sci Adv*. 2022;8(38):eabn3181. doi:10.1126/sciadv.abn3181
53. Kang K, Watanabe S, Broch K, et al. 2D coherent charge transport in highly ordered conducting polymers doped by solid state diffusion. *Nat Mater*. 2016;15(8):896-902. doi:10.1038/nmat4634
54. Qian F, Hu M, Gong J, et al. Enhanced thermoelectric performance in lead-free inorganic CsSn1−xGexI3 perovskite semiconductors. *J Phys Chem C*. 2020;124(22):11749-11753. doi:10.1021/acs.jpcc.0c00459
55. Chen M, Ju MG, Garces HF, et al. Highly stable and efficient all-inorganic lead-free perovskite solar cells with native-oxide passivation. *Nat Commun*. 2019;10(1):16. doi:10.1038/s41467-018-07951-y
56. Wang Q, Shao Y, Xie H, et al. Qualifying composition dependent p and n self-doping in CH3NH3PbI3. *Appl Phys Lett*. 2014;105(16):163508. doi:10.1063/1.4899051
57. Liu Q, Hsiao YC, Ahmadi M, et al. N and p-type properties in organo-metal halide perovskites studied by Seebeck effects. *Org Electron*. 2016;35:216-220. doi:10.1016/j.orgel.2016.05.025
58. Wu T, Mukherjee R, Ovchinnikova OS, et al. Metal/ion interactions induced p–i–n junction in methylammonium lead triiodide perovskite single crystals. *J Am Chem Soc*. 2017;139(48):17285-17288. doi:10.1021/jacs.7b10416
59. Xie Z, Feng K, Xiong Y, et al. A high seebeck voltage thermoelectric module with P-type and N-type MAPbI3 perovskite single crystals. *Adv Electron Mater*. 2021;7(3):2001003. doi:10.1002/aelm.202001003
60. Yin WJ, Shi T, Yan Y. Unusual defect physics in CH3NH3PbI3 perovskite solar cell absorber. *Appl Phys Lett*. 2014;104(6):063903. doi:10.1063/1.4864778
61. Lin CH, Hu L, Guan X, et al. Electrode engineering in halide perovskite electronics: plenty of room at the interfaces. *Adv Mater*. 2022;34(18):2108616. doi:10.1002/adma.202108616

62. Goldschmidt VM. Die gesetze der krystallochemie. *Naturwissenschaften*. 1926;14(21):477-485. doi:10.1007/BF01507527
63. Shahbazi S, Tsai CM, Narra S, et al. Ag doping of organometal lead halide perovskites: morphology modification and p-type character. *J Phys Chem C*. 2017;121(7):3673-3679. doi:10.1021/acs.jpcc.6b09722
64. Abdi-Jalebi M, Pazoki M, Philippe B, et al. Dedoping of lead halide perovskites incorporating monovalent cations. *ACS Nano*. 2018;12(7):7301-7311. doi:10.1021/acsnano.8b03586
65. Lin Y, Shao Y, Dai J, et al. Metallic surface doping of metal halide perovskites. *Nat Commun*. 2021;12(1):7. doi:10.1038/s41467-020-20110-6
66. Xiong Y, Xu L, Wu P, Sun L, Xie G, Hu B. Bismuth doping–induced stable seebeck effect based on MAPbI3 polycrystalline thin films. *Adv Funct Mater*. 2019;29(16):1900615. doi:10.1002/adfm.201900615
67. Tang W, Zhang J, Ratnasingham S, et al. Substitutional doping of hybrid organic–inorganic perovskite crystals for thermoelectrics. *J Mater Chem A Mater*. 2020;8(27):13594-13599. doi:10.1039/D0TA03648J
68. Salzmann I, Heimel G, Oehzelt M, Winkler S, Koch N. Molecular electrical doping of organic semiconductors: fundamental mechanisms and emerging dopant design rules. *Acc Chem Res*. 2016;49(3):370-378. doi:10.1021/acs.accounts.5b00438
69. Kim TH, Kim JH, Kang K. Molecular doping principles in organic electronics: fundamentals and recent progress. *Jpn J Appl Phys*. 2023;62:SE0803. doi:10.35848/1347-4065/acbb10
70. Song D, Wei D, Cui P, et al. Dual function interfacial layer for highly efficient and stable lead halide perovskite solar cells. *J Mater Chem A Mater*. 2016;4(16):6091-6097. doi:10.1039/C6TA00577B
71. Reo Y, Zhu H, Liu A, Noh YY. Molecular doping enabling mobility boosting of 2D Sn2+-based perovskites. *Adv Funct Mater*. 2022;32(38):2204870. doi:10.1002/adfm.202204870
72. Noel NK, Habisreutinger SN, Pellaroque A, et al. Interfacial charge-transfer doping of metal halide perovskites for high performance photovoltaics. *Energ Environ Sci*. 2019;12(10):3063-3073. doi:10.1039/C9EE01773A
73. Perry EE, Labram JG, Venkatesan NR, Nakayama H, Chabinyc ML. N-type surface doping of MAPbI3 via charge transfer from small molecules. *Adv Electron Mater*. 2018;4(7):1800087. doi:10.1002/aelm.201800087
74. Zheng L, Zhu T, Li Y, et al. Enhanced thermoelectric performance of F4-TCNQ doped FASnI3 thin films. *J Mater Chem A Mater*. 2020;8(47):25431-25442. doi:10.1039/D0TA09329G
75. Ghosh D, Welch E, Neukirch AJ, Zakhidov A, Tretiak S. Polarons in halide perovskites: a perspective. *J Phys Chem Lett*. 2020;11(9):3271-3286. doi:10.1021/acs.jpclett.0c00018
76. Yamada Y, Kanemitsu Y. Electron-phonon interactions in halide perovskites. *NPG Asia Mater*. 2022;14(1):48. doi:10.1038/s41427-022-00394-4
77. Brenner TM, Egger DA, Kronik L, Hodes G, Cahen D. Hybrid organic—inorganic perovskites: low-cost semiconductors with intriguing charge-transport properties. *Nat Rev Mater*. 2016;1(1):15007. doi:10.1038/natrevmats.2015.7
78. Schilcher MJ, Robinson PJ, Abramovitch DJ, et al. The significance of polarons and dynamic disorder in halide perovskites. *ACS Energy Lett*. 2021;6(6):2162-2173. doi:10.1021/acsenergylett.1c00506
79. Brenner TM, Egger DA, Rappe AM, Kronik L, Hodes G, Cahen D. Are mobilities in hybrid organic–inorganic halide perovskites actually "high"? *J Phys Chem Lett*. 2015;6(23):4754-4757. doi:10.1021/acs.jpclett.5b02390
80. Mahata A, Meggiolaro D, De Angelis F. From large to small polarons in lead, tin, and mixed lead–tin halide perovskites. *J Phys Chem Lett*. 2019;10(8):1790-1798. doi:10.1021/acs.jpclett.9b00422
81. Miyata K, Meggiolaro D, Trinh MT, et al. Large polarons in lead halide perovskites. *Sci Adv*. 2017;3(8):e1701217. doi:10.1126/sciadv.1701217
82. Neukirch AJ, Nie W, Blancon JC, et al. Polaron stabilization by cooperative lattice distortion and cation rotations in hybrid perovskite materials. *Nano Lett*. 2016;16(6):3809-3816. doi:10.1021/acs.nanolett.6b01218
83. Park M, Neukirch AJ, Reyes-Lillo SE, et al. Excited-state vibrational dynamics toward the polaron in methylammonium lead iodide perovskite. *Nat Commun*. 2018;9(1):2525. doi:10.1038/s41467-018-04946-7
84. Zheng F, Wang LW. Large polaron formation and its effect on electron transport in hybrid perovskites. *Energy Environ Sci*. 2019;12(4):1219-1230. doi:10.1039/C8EE03369B
85. Yaffe O, Guo Y, Tan LZ, et al. Local polar fluctuations in lead halide perovskite crystals. *Phys Rev Lett*. 2017;118(13):136001. doi:10.1103/PhysRevLett.118.136001
86. Lee S, Nathan A, Robertson J, et al. Temperature dependent electron transport in amorphous oxide semiconductor thin film transistors. 2011 International Electron Devices Meeting; 2011:14.6.1–14.6.4. doi:10.1109/IEDM.2011.6131554
87. Sakanoue T, Sirringhaus H. Band-like temperature dependence of mobility in a solution-processed organic semiconductor. *Nat Mater*. 2010;9(9):736-740. doi:10.1038/nmat2825
88. Ganose AM, Park J, Jain A. The temperature-dependence of carrier mobility is not a reliable indicator of the dominant scattering mechanism. arXiv preprint arXiv:221001746. 2022.
89. Milot RL, Eperon GE, Snaith HJ, Johnston MB, Herz LM. Temperature-dependent charge-carrier dynamics in CH3NH3PbI3 perovskite thin films. *Adv Funct Mater*. 2015;25(39):6218-6227. doi:10.1002/adfm.201502340
90. Karakus M, Jensen SA, D'Angelo F, Turchinovich D, Bonn M, Cánovas E. Phonon–electron scattering limits free charge mobility in methylammonium lead iodide perovskites. *J Phys Chem Lett*. 2015;6(24):4991-4996. doi:10.1021/acs.jpclett.5b02485
91. Oga H, Saeki A, Ogomi Y, Hayase S, Seki S. Improved understanding of the electronic and energetic landscapes of perovskite solar cells: high local charge carrier mobility, reduced recombination, and extremely shallow traps. *J Am Chem Soc*. 2014;136(39):13818-13825. doi:10.1021/ja506936f
92. Sendner M, Nayak PK, Egger DA, et al. Optical phonons in methylammonium lead halide perovskites and implications for charge transport. *Mater Horiz*. 2016;3(6):613-620. doi:10.1039/C6MH00275G
93. Miyata K, Zhu XY. Ferroelectric large polarons. *Nat Mater*. 2018;17(5):379-381. doi:10.1038/s41563-018-0068-7
94. Frost JM. Calculating polaron mobility in halide perovskites. *Phys Rev B*. 2017;96(19):195202. doi:10.1103/PhysRevB.96.195202
95. Mayers MZ, Tan LZ, Egger DA, Rappe AM, Reichman DR. How lattice and charge fluctuations control carrier dynamics in halide perovskites. *Nano Lett*. 2018;18(12):8041-8046. doi:10.1021/acs.nanolett.8b04276

96. Phung N, Félix R, Meggiolaro D, et al. The doping mechanism of halide perovskite unveiled by alkaline earth metals. *J Am Chem Soc*. 2020;142(5):2364-2374. doi:10.1021/jacs.9b11637
97. Zhao Y, Yavuz I, Wang M, et al. Suppressing ion migration in metal halide perovskite via interstitial doping with a trace amount of multivalent cations. *Nat Mater*. 2022;21(12):1396-1402. doi:10.1038/s41563-022-01390-3
98. Euvrard J, Gunawan O, Zhong X, Harvey SP, Kahn A, Mitzi DB. p-Type molecular doping by charge transfer in halide perovskite. *Mater Adv*. 2021;2(9):2956-2965. doi:10.1039/D1MA00160D
99. Barker AJ, Sadhanala A, Deschler F, et al. Defect-assisted photoinduced halide segregation in mixed-halide perovskite thin films. *ACS Energy Lett*. 2017;2(6):1416-1424. doi:10.1021/acsenergylett.7b00282
100. Zhu H, Liu A, Shim KI, Hong J, Han JW, Noh YY. High-performance and reliable lead-free layered-perovskite transistors. *Adv Mater*. 2020;32(31):2002717. doi:10.1002/adma.202002717
101. Lee J, Baek KY, Lee J, et al. Bulk incorporation of molecular dopants into Ruddlesden–popper organic metal–halide perovskites for charge transfer doping. *Adv Funct Mater*. 2023;2302048. Published Online May 12. doi:10.1002/adfm.202302048
102. Chen X, Parker D, Singh DJ. Importance of non-parabolic band effects in the thermoelectric properties of semiconductors. *Sci Rep*. 2013;3(1):3168. doi:10.1038/srep03168
103. Sootsman JR, Chung DY, Kanatzidis MG. New and old concepts in thermoelectric materials. *Angew Chem Int Ed*. 2009;48(46):8616-8639. doi:10.1002/anie.200900598
104. Conings B, Drijkoningen J, Gauquelin N, et al. Intrinsic thermal instability of methylammonium lead trihalide perovskite. *Adv Energy Mater*. 2015;5(15):1500477. doi:10.1002/aenm.201500477
105. Alotaibi NH, Mustafa GM, Kattan NA, et al. DFT study of double perovskites Cs2AgBiX6 (X = Cl, Br): an alternative of hybrid perovskites. *J Solid State Chem*. 2022;313:123353. doi:10.1016/j.jssc.2022.123353
106. Tariq M, Ali MA, Laref A, Murtaza G. Anion replacement effect on the physical properties of metal halide double perovskites Cs2AgInX6 (X = F, Cl, Br, I). *Solid State Commun*. 2020;314-315:113929. doi:10.1016/j.ssc.2020.113929
107. Yang SJ, Kim D, Choi J, et al. Enhancing thermoelectric power factor of 2D organometal halide perovskites by suppressing 2D/3D phase separation. *Adv Mater*. 2021;33(38):2102797. doi:10.1002/adma.202102797
108. Hsu SN, Zhao W, Gao Y, et al. Thermoelectric performance of lead-free two-dimensional halide perovskites featuring conjugated ligands. *Nano Lett*. 2021;21(18):7839-7844. doi:10.1021/acs.nanolett.1c02890
109. Ghosh T, Dutta M, Sarkar D, Biswas K. Insights into low thermal conductivity in inorganic materials for thermoelectrics. *J Am Chem Soc*. 2022;144(23):10099-10118. doi:10.1021/jacs.2c02017
110. Pei Y, Wang H, Snyder GJ. Band engineering of thermoelectric materials. *Adv Mater*. 2012;24(46):6125-6135. doi:10.1002/adma.201202919
111. Lee HD, Kim H, Cho H, et al. Efficient Ruddlesden–popper perovskite light-emitting diodes with randomly oriented nanocrystals. *Adv Funct Mater*. 2019;29(27):1901225. doi:10.1002/adfm.201901225
112. Chen B, Yang M, Priya S, Zhu K. Origin of J–V hysteresis in perovskite solar cells. *J Phys Chem Lett*. 2016;7(5):905-917. doi:10.1021/acs.jpclett.6b00215
113. Eames C, Frost JM, Barnes PRF, O'Regan BC, Walsh A, Islam MS. Ionic transport in hybrid lead iodide perovskite solar cells. *Nat Commun*. 2015;6(1):7497. doi:10.1038/ncomms8497
114. Wang J, Senanayak SP, Liu J, et al. Investigation of electrode electrochemical reactions in CH3NH3PbBr3 perovskite single-crystal field-effect transistors. *Adv Mater*. 2019;31(35):1902618. doi:10.1002/adma.201902618
115. Sun S, Li M, Shi XL, Chen ZG. Advances in ionic thermoelectrics: from materials to devices. *Adv Energy Mater*. 2023;13(9):2203692. doi:10.1002/aenm.202203692
116. Fu J, Xu Q, Han G, et al. Hot carrier cooling mechanisms in halide perovskites. *Nat Commun*. 2017;8(1):1300. doi:10.1038/s41467-017-01360-3
117. Stranks SD, Eperon GE, Grancini G, et al. Electron-hole diffusion lengths exceeding 1 micrometer in an organometal trihalide perovskite absorber. *Science*. 2013;342(6156):341-344. doi:10.1126/science.1243982
118. Li Z, Jia B, Fang S, et al. Pressure-tuning photothermal synergy to optimize the photoelectronic properties in amorphous halide perovskite Cs3Bi2I9. *Adv Sci*. 2023;10(6):2205837. doi:10.1002/advs.202205837
119. Zhou Y, Yin X, Zhang Q, et al. Perovskite solar cell-thermoelectric tandem system with a high efficiency of over 23%. *Mater Today Energy*. 2019;12:363-370. doi:10.1016/j.mtener.2019.03.003
120. Venkatasubramanian R, Siivola E, Colpitts T, O'Quinn B. Thin-film thermoelectric devices with high room-temperature figures of merit. *Nature*. 2001;413(6856):597-602. doi:10.1038/35098012
121. Snyder GJ, Christensen M, Nishibori E, Caillat T, Iversen BB. Disordered zinc in Zn4Sb3 with phonon-glass and electron-crystal thermoelectric properties. *Nat Mater*. 2004;3(7):458-463. doi:10.1038/nmat1154
122. Rogl G, Grytsiv A, Rogl P, et al. n-Type skutterudites (R, Ba, Yb) yCo4Sb12 (R = Sr, La, Mm, DD, SrMm, SrDD) approaching ZT ≈ 2.0. *Acta Mater*. 2014;63:30-43. doi:10.1016/j.actamat.2013.09.039
123. Xie W, He J, Kang HJ, et al. Identifying the specific nanostructures responsible for the high thermoelectric performance of $(Bi,Sb)_2Te_3$ nanocomposites. *Nano Lett*. 2010;10(9):3283-3289. doi:10.1021/nl100804a
124. Joshi G, Lee H, Lan Y, et al. Enhanced thermoelectric figure-of-merit in nanostructured p-type silicon germanium bulk alloys. *Nano Lett*. 2008;8(12):4670-4674. doi:10.1021/nl8026795
125. Zhao LD, Hao S, Lo SH, et al. High thermoelectric performance via hierarchical compositionally alloyed nanostructures. *J Am Chem Soc*. 2013;135(19):7364-7370. doi:10.1021/ja403134b
126. Fujita I, Kishimoto K, Sato M, Anno H, Koyanagi T. Thermoelectric properties of sintered clathrate compounds Sr8GaxGe46−x with various carrier concentrations. *J Appl Phys*. 2006;99(9):093707. doi:10.1063/1.2194187
127. Wang L, Chen LD, Chen XH, Zhang WB. Synthesis and thermoelectric properties of n-type Sr8Ga16−xGe30−y clathrates with different Ga/Ge ratios. *J Phys D Appl Phys*. 2009;42(4):045113. doi:10.1088/0022-3727/42/4/045113

128. Chen LD, Kawahara T, Tang XF, et al. Anomalous barium filling fraction and n-type thermoelectric performance of BayCo4Sb12. *J Appl Phys*. 2001;90(4):1864-1868. doi:10.1063/1.1388162
129. Wang XW, Lee H, Lan YC, et al. Enhanced thermoelectric figure of merit in nanostructured n-type silicon germanium bulk alloy. *Appl Phys Lett*. 2008;93(19):193121. doi:10.1063/1.3027060
130. Pei Y, Shi X, LaLonde A, Wang H, Chen L, Snyder GJ. Convergence of electronic bands for high performance bulk thermoelectrics. *Nature*. 2011;473(7345):66-69. doi:10.1038/nature09996
131. Biswas K, He J, Blum ID, et al. High-performance bulk thermoelectrics with all-scale hierarchical architectures. *Nature*. 2012;489(7416):414-418. doi:10.1038/nature11439
132. Martin J, Wang H, Nolas GS. Optimization of the thermoelectric properties of Ba8Ga16Ge30. *Appl Phys Lett*. 2008;92(22):222110. doi:10.1063/1.2939438
133. Yang D, Su X, Li J, et al. Blocking ion migration stabilizes the high thermoelectric performance in Cu2Se composites. *Adv Mater*. 2020;32(40):2003730. doi:10.1002/adma.202003730
134. Shi X, Kong H, Li CP, et al. Low thermal conductivity and high thermoelectric figure of merit in n-type BaxYbyCo4Sb12 double-filled skutterudites. *Appl Phys Lett*. 2008;92(18):182101. doi:10.1063/1.2920210
135. He Y, Lu P, Shi X, et al. Ultrahigh thermoelectric performance in mosaic crystals. *Adv Mater*. 2015;27(24):3639-3644. doi:10.1002/adma.201501030
136. Liu H, Shi X, Xu F, et al. Copper ion liquid-like thermoelectrics. *Nat Mater*. 2012;11(5):422-425. doi:10.1038/nmat3273
137. Rhyee JS, Lee KH, Lee SM, et al. Peierls distortion as a route to high thermoelectric performance in In4Se3-δ crystals. *Nature*. 2009;459(7249):965-968. doi:10.1038/nature08088
138. Liu H, Yuan X, Lu P, et al. Ultrahigh thermoelectric performance by electron and phonon critical scattering in Cu2Se1-xIx. *Adv Mater*. 2013;25(45):6607-6612. doi:10.1002/adma.201302660
139. He Y, Day T, Zhang T, et al. High thermoelectric performance in non-toxic earth-abundant copper sulfide. *Adv Mater*. 2014;26(23):3974-3978. doi:10.1002/adma.201400515
140. Chang C, Wu M, He D, et al. 3D charge and 2D phonon transports leading to high out-of-plane ZT in n-type SnSe crystals. *Science*. 2018;360(6390):778-783. doi:10.1126/science.aaq1479
141. Il KS, Lee KH, Mun HA, et al. Dense dislocation arrays embedded in grain boundaries for high-performance bulk thermoelectrics. *Science*. 2015;348(6230):109-114. doi:10.1126/science.aaa4166
142. Shi X, Yang J, Bai S, et al. On the design of high-efficiency thermoelectric clathrates through a systematic cross-substitution of framework elements. *Adv Funct Mater*. 2010;20(5):755-763. doi:10.1002/adfm.200901817
143. Sales BC, Mandrus D, Williams RK. Filled skutterudite antimonides: a new class of thermoelectric materials. *Science*. 1996;272(5266):1325-1328. doi:10.1126/science.272.5266.1325
144. Jiang B, Yu Y, Cui J, et al. High-entropy-stabilized chalcogenides with high thermoelectric performance. *Science*. 2021;371(6531):830-834. doi:10.1126/science.abe1292
145. Hsu KF, Loo S, Guo F, et al. Cubic AgPbmSbTe2+m: bulk thermoelectric materials with high figure of merit. *Science*. 2004;303(5659):818-821. doi:10.1126/science.1092963
146. Wang J, Cai K, Shen S. A facile chemical reduction approach for effectively tuning thermoelectric properties of PEDOT films. *Org Electron*. 2015;17:151-158. doi:10.1016/j.orgel.2014.12.007
147. Huang D, Wang C, Zou Y, et al. Bismuth interfacial doping of organic small molecules for high performance n-type thermoelectric materials. *Angew Chem Int Ed*. 2016;55(36):10672-10675. doi:10.1002/anie.201604478
148. Bubnova O, Khan ZU, Malti A, et al. Optimization of the thermoelectric figure of merit in the conducting polymer poly(3,-4-ethylenedioxythiophene). *Nat Mater*. 2011;10(6):429-433. doi:10.1038/nmat3012
149. Qu S, Yao Q, Wang L, et al. Highly anisotropic P3HT films with enhanced thermoelectric performance via organic small molecule epitaxy. *NPG Asia Mater*. 2016;8(7):e292. doi:10.1038/am.2016.97
150. Fan Z, Du D, Guan X, Ouyang J. Polymer films with ultrahigh thermoelectric properties arising from significant seebeck coefficient enhancement by ion accumulation on surface. *Nano Energy*. 2018;51:481-488. doi:10.1016/j.nanoen.2018.07.002
151. Liu J, van der Zee B, Alessandri R, et al. N-type organic thermoelectrics: demonstration of ZT > 0.3. *Nat Commun*. 2020;11(1):5694. doi:10.1038/s41467-020-19537-8
152. Sun Y, Sheng P, Di C, et al. Organic thermoelectric materials and devices based on p- and n-type poly(metal 1,1,2,2-ethenetetrathiolate)s. *Adv Mater*. 2012;24(7):932-937. doi:10.1002/adma.201104305
153. Lee SH, Park H, Kim S, Son W, Cheong IW, Kim JH. Transparent and flexible organic semiconductor nanofilms with enhanced thermoelectric efficiency. *J Mater Chem A Mater*. 2014;2(20):7288-7294. doi:10.1039/C4TA00700J
154. Culebras M, Gómez CM, Cantarero A. Enhanced thermoelectric performance of PEDOT with different counter-ions optimized by chemical reduction. *J Mater Chem A Mater*. 2014;2(26):10109-10115. doi:10.1039/C4TA01012D
155. Lee SH, Park H, Son W, Choi HH, Kim JH. Novel solution-processable, dedoped semiconductors for application in thermoelectric devices. *J Mater Chem A Mater*. 2014;2(33):13380-13387. doi:10.1039/C4TA01839G
156. Bubnova O, Berggren M, Crispin X. Tuning the thermoelectric properties of conducting polymers in an electrochemical transistor. *J Am Chem Soc*. 2012;134(40):16456-16459. doi:10.1021/ja305188r
157. Huang D, Yao H, Cui Y, et al. Conjugated-backbone effect of organic small molecules for n-type thermoelectric materials with ZT over 0.2. *J Am Chem Soc*. 2017;139(37):13013-13023. doi:10.1021/jacs.7b05344
158. Baranwal AK, Saini S, Wang Z, et al. Interface engineering using Y2O3 scaffold to enhance the thermoelectric performance of CsSnI3 thin film. *Org Electron*. 2020;76:105488. doi:10.1016/j.orgel.2019.105488
159. Mettan X, Pisoni R, Matus P, et al. Tuning of the thermoelectric figure of merit of CH3NH3MI3 (M=Pb,Sn) photovoltaic perovskites. *J Phys Chem C*. 2015;119(21):11506-11510. doi:10.1021/acs.jpcc.5b03939
160. Baranwal AK, Saini S, Sanehira Y, et al. Unveiling the role of the metal oxide/Sn perovskite Interface leading to low efficiency of Sn-perovskite solar cells but providing high thermoelectric properties. *ACS Appl Energy Mater*. 2022;5(8):9750-9758. doi:10.1021/acsaem.2c01437
161. Saini S, Baranwal AK, Yabuki T, Hayase S, Miyazaki K. Growth of halide perovskites thin films for thermoelectric

applications. *MRS Adv*. 2019;4(30):1719-1725. doi:10.1557/adv.2019.279

162. Sebastia-Luna P, Pokharel U, Huisman BAH, Koster LJA, Palazon F, Bolink HJ. Vacuum-deposited cesium tin iodide thin films with tunable thermoelectric properties. *ACS Appl Energy Mater*. 2022;5(8):10216-10223. doi:10.1021/acsaem.2c01936

AUTHOR BIOGRAPHIES

Yongjin Kim received his BS degree in Physics and Materials Science and Engineering as a double major from Yonsei University, South Korea. He is currently a PhD student in the Department of Materials Science and Engineering at Seoul National University, South Korea. His recent research interests focus on the electrical doping and electronics of metal halide perovskites.

Takhee Lee is a professor at Department of Physics and Astronomy at Seoul National University (SNU), South Korea. He received his BS and MS degree in physics at SNU, South Korea in 1992 and 1994, respectively, and he received his PhD degree in physics at Purdue University, USA in 2000. He was a post doctor at Yale University, USA until 2004. His current research at SNU is characterization of the electrical properties of structures involving single molecules, self-assembled monolayers, polymers, perovskites, and semiconductor nanomaterials, and their assembly into electronic devices.

Keehoon Kang is an assistant professor at Department of Materials Science and Engineering at Seoul National University, South Korea. He received BA & MSci (combined) and PhD degrees from University of Cambridge in 2012 and 2017, respectively. After his postdoctoral research position at Department of Physics at Seoul National University, he joined the Department of Materials Science and Engineering at Yonsei University as a faculty member from 2021 to 2022. His research interests range from the materials and device physics of organic and hybrid electronic materials.

SUPPORTING INFORMATION

Additional supporting information can be found online in the Supporting Information section at the end of this article.

How to cite this article: Kim Y, Choi H, Lee J, et al. Unlocking the potential of metal halide perovskite thermoelectrics through electrical doping: A critical review. *EcoMat*. 2023;5(11): e12406. doi:10.1002/eom2.12406